Aspen SUCROSE TRANSPORTER3 Allocates Carbon into Wood Fibers[1][C][W]

Amir Mahboubi, Christine Ratke, András Gorzsás, Manoj Kumar[2], Ewa J. Mellerowicz, and Totte Niittylä*

Umeå Plant Science Centre, Department of Forest Genetics and Plant Physiology, Swedish University of Agricultural Sciences, SE 90183 Umea, Sweden (A.M., C.R., M.K., E.J.M., T.N.); and Department of Chemistry, Umeå University, SE 90187 Umea, Sweden (A.G.)

ORCID ID: 0000-0001-8029-1503 (T.N.).

Wood formation in trees requires carbon import from the photosynthetic tissues. In several tree species, including *Populus* species, the majority of this carbon is derived from sucrose (Suc) transported in the phloem. The mechanism of radial Suc transport from phloem to developing wood is not well understood. We investigated the role of active Suc transport during secondary cell wall formation in hybrid aspen (*Populus tremula* × *Populus tremuloides*). We show that RNA interference-mediated reduction of *PttSUT3* (for Suc/H^+ symporter) during secondary cell wall formation in developing wood caused thinner wood fiber walls accompanied by a reduction in cellulose and an increase in lignin. Suc content in the phloem and developing wood was not significantly changed. However, after $^{13}CO_2$ assimilation, the *SUT3RNAi* lines contained more ^{13}C than the wild type in the Suc-containing extract of developing wood. Hence, Suc was transported into developing wood, but the Suc-derived carbon was not efficiently incorporated to wood fiber walls. A yellow fluorescent protein:PttSUT3 fusion localized to plasma membrane, suggesting that reduced Suc import into developing wood fibers was the cause of the observed cell wall phenotype. The results show the importance of active Suc transport for wood formation in a symplasmically phloem-loading tree species and identify PttSUT3 as a principal transporter for carbon delivery into secondary cell wall-forming wood fibers.

In trees, the majority of the assimilated carbon dioxide accounting for biomass increase is deposited in the secondary cell walls of wood. In several tree species, most of this carbon is derived from Suc imported from leaves (Turgeon, 1996). Suc transport from leaves to wood occurs in the phloem sieve elements, where a pressure flow mechanism is thought to drive the movement of solutes from source to sink tissues (Münch, 1930; Knoblauch and Peters, 2010). In Münch's pressure flow model, a high source tissue solute concentration causes an osmotic pressure driving the uptake of water and a subsequent flow of water and solutes toward sink tissues with lower solute concentration and osmotic pressure. In most tree species, including *Populus* spp., phloem loading is thought to occur passively through the symplasm (Davidson et al., 2011; Fu et al., 2011). In this process, Suc is thought to move passively by diffusion through plasmodesmata connecting mesophyll cells and into the phloem sieve element/companion cells of the source leaves. In addition to phloem loading in leaves, the maintenance of the source-to-sink flow requires that the sink tissues are actively lowering the phloem solute concentration either through metabolism or export (Münch, 1930; Van Bel, 2003). Therefore, it can be hypothesized that active Suc transport from the phloem into developing wood may be important for wood formation in Suc-transporting trees.

Our knowledge of the molecular mechanisms involved in the radial phloem-to-developing wood Suc transport is very limited. In trees, this transport of Suc is thought to occur mainly through ray cells. Ray cells are symplasmically connected parenchyma cells that have an important function in the nutrient exchange between phloem and wood (Van Bel, 1990). Symplasmic connections between phloem and ray cells appear to be rare in most investigated plant species (Van Bel, 1990). However, in *Populus* × *canadensis* wood, symplasmic phloem-to-ray transport appeared to dominate (Sauter and Kloth, 1986). Sauter and Kloth (1986) estimated the minimum radial carbon flux rate from the rate of starch accumulation in ray cells, concluding that only a symplasmic radial carbon transport route could explain the observed starch accumulation rates. Additional support for the predominance of the wood ray cell route in phloem unloading was provided by stem section autoradiographs of $^{14}CO_2$-labeled 2-year-old spruce (*Picea* spp.) trees showing clear labeling of ray cells (Langenfeld-Heyser, 1987).

The export of solutes from ray cells to the developing wood is thought to occur primarily across so-called contact pits located between ray cells and fibers (Barnett, 1981; Van Bel, 1990). The mature pits are spherical porous openings crossing the cell walls of two neighboring

[1] This work was supported by the Swedish Research Council FORMAS (Bioimprove), VINNOVA, Trees and Crops for the Future, and Bio4Energy, the Swedish program for renewable energy.

[2] Present address: Faculty of Life Sciences, University of Manchester, Manchester M13 9PT, United Kingdom.

* Address correspondence to totte.niittyla@slu.se.

The author responsible for distribution of materials integral to the findings presented in this article in accordance with the policy described in the Instructions for Authors (www.plantphysiol.org) is: Totte Niittylä (totte.niittyla@slu.se).

[C] Some figures in this article are displayed in color online but in black and white in the print edition.

[W] The online version of this article contains Web-only data.
www.plantphysiol.org/cgi/doi/10.1104/pp.113.227603

cells, allowing solute transport between lignified cells, whereas developing pits have been observed to contain symplasmic connections in some species but not in others (Barnett, 1981). For example, electron microscopy images of differentiating tracheids in *Pinus radiata* wood did not show symplasmic connections (Barnett and Harris, 1975), whereas clear connections were documented in the developing fiber pits of *Aesculus hippocastanum* (Barnett, 1981). Anatomical studies of the developing pit structure in *Populus* spp. are limited, but investigation of symplasmic connectivity in the developing wood of hybrid aspen (*Populus tremula* × *Populus tremuloides*) using symplasmic fluorescent tracers did not reveal connections between rays and developing vessels and fibers (Sokołowska and Zagórska-Marek, 2012). This observation suggested that, during wood formation, Suc is exported across the ray cell plasma membrane and imported across the plasma membrane of the developing fibers and vessels. Thus, at least in *Populus* spp., this step in the radial wood Suc import pathway may involve active transport.

Suc/H^+ symporters (SUTs) facilitating active Suc import into cytosol have been identified in several plant species (Lalonde et al., 2004; Kühn and Grof, 2010). According to the current nomenclature, SUTs are classified into groups I to IV based on their phylogenetic relationship (Sauer, 2007). The sequenced *Populus trichocarpa* genome encodes for five functional SUTs representing group II (PtSUT1 and PtSUT3), group III (PtSUT5 and PtSUT6), and group IV (PtSUT4; Payyavula et al., 2011). Quantitative reverse transcription-PCR (qPCR) analysis of *SUT* transcript levels in greenhouse-grown *Populus tremula* × *Populus alba* showed *PtaSUT1* transcripts in phloem and roots, *PtaSUT3* transcripts primarily in stems undergoing secondary growth, and *PtaSUT4*, *PtaSUT5*, and *PtaSUT6* transcripts ubiquitously throughout the tree (Payyavula et al., 2011). Interestingly, microarray transcript profiling of different wood developmental stages in greenhouse-grown hybrid aspen showed an increase in *PttSUT1* and/or *PttSUT3* transcript levels during secondary cell wall formation (Hertzberg et al., 2001). The coding sequences of *PttSUT1* and *PttSUT3* are 90% identical; hence, the complementary DNA microarray probe may have hybridized to both transcripts. The expression patterns of the other *PttSUTs* during wood formation is not known, since the microarray used by Hertzberg et al. (2001) only included a probe for *PttSUT1/PttSUT3*.

Of the *Populus* spp. *SUTs*, only *PtaSUT4* has been studied in detail. Similar to orthologous group IV SUTs from barley (*Hordeum vulgare*) and Arabidopsis (*Arabidopsis thaliana*; Endler et al., 2006; Schneider et al., 2012), a GFP:PtaSUT4 fusion protein was localized to the vacuolar tonoplast membrane in tobacco (*Nicotiana tabacum*) protoplasts (Payyavula et al., 2011). In agreement with the qPCR results, in situ hybridization of *PtaSUT4* transcripts in source leaf lamina and stem cross sections showed a clear signal, supporting a role for *PtaSUT4* in Suc transport in these tissues. Reduction of *PtaSUT4* expression in greenhouse-grown *P. tremula* × *P. alba* using a *35S* promoter-driven *SUT4RNAi* construct resulted in Suc accumulation in source leaves, phloem, and developing wood (Payyavula et al., 2011). No effect on wood anatomy or biosynthesis was reported for the *PtaSUT4RNAi* lines, but the lines did show a modest reduction in total shoot biomass (Payyavula et al., 2011). Payyavula et al. (2011) interpreted the *PtaSUT4RNAi* phenotype to reflect an important role of tonoplast Suc transport in the modulation of Suc export from leaves as well as the maintenance of Suc homeostasis in sink tissues.

To explore the role of active Suc transport in the radial phloem-to-wood pathway, we first quantified transcript levels of all *P. tremula SUTs* at different wood developmental stages from cambium to maturation/cell death. This analysis established that the previously observed increase in *PttSUT1* and/or *PttSUT3* transcript levels during secondary cell wall formation (Hertzberg et al., 2001) was due to *PttSUT3*. The group II SUTs, to which also *Populus* spp. SUT3 belongs, have been mainly associated with phloem loading and transport in apoplasmically loading species such as potato (*Solanum tuberosum*), tobacco, and Arabidopsis (Riesmeier et al., 1994; Burkle et al., 1998; Gottwald et al., 2000). However, the function of group II SUTs in symplasmic phloem loaders such as *Populus* spp. has not been investigated, nor has the role of SUTs during secondary cell wall biosynthesis in wood. To examine the function of *Populus* spp. SUT3 during wood formation, we generated transgenic hybrid aspen *SUT3RNAi* lines, where the RNA interference construct was expressed under the control of a promoter driving expression during secondary cell wall formation. Reduction of *PttSUT3* transcript levels in developing wood led to decreased carbon allocation to secondary cell walls, as shown by thinner fiber cell walls, while at the same time the accumulation of ^{13}C in developing wood after $^{13}CO_2$ supply was not reduced. Thus, our results supported a central role for *Populus* spp. SUT3 in Suc import to secondary cell wall-forming wood fibers.

RESULTS

Characterization of *SUT* Expression during Wood Formation

The *P. trichocarpa* genome encodes for five Suc transporters (*PtSUT1*, *PtSUT3*, *PtSUT4*, *PtSUT5*, and *PtSUT6*; Payyavula et al., 2011). To investigate the expression of *Populus* spp. *SUTs* at different stages of wood formation, we analyzed *SUT* transcript levels in cambium, early expansion, late expansion, secondary cell wall, and maturation/cell death zones using qPCR. Samples were harvested from approximately 45-year-old *P. tremula* trees on July 7, 2010, at Mullkälen, Sweden. Anatomical inspection and viability staining of wood showed that all trees were undergoing active wood formation (Supplemental Fig. S1). Total RNA from frozen microtome-cut sections corresponding to cambium, early expansion, late expansion, secondary cell wall, and maturation/cell

death zones was isolated from three independent trees. qPCR with gene-specific primers showed *PtSUT1* transcript levels to be low in the cambium and below detection in the developing wood. *PtSUT4*, *PtSUT5*, and *PtSUT6* transcript levels were stable across the developing wood, while *PtSUT3* transcripts were highest in the cambium, low in the early expansion zone, and increased in the late expansion zone to peak during secondary cell wall formation (Fig. 1). The latter observation suggested a role for *PtSUT3* in Suc transport to secondary cell wall-forming cells.

Populus Spp. SUT3 Is a Plasma Membrane-Localized Suc Transporter

Populus spp. SUT3 (POPTR_0019s11560) is a functional Suc transporter, as shown by a previous study where *P. tremula* × *P. alba SUT3* complemented a yeast mutant deficient in Suc uptake from the growth medium (Payyavula et al., 2011). In our work, we used the hybrid aspen as a model system to investigate *PttSUT3* function during secondary cell wall biosynthesis. To determine the subcellular location of *PttSUT3*, a yellow fluorescent protein (*YFP*):*PttSUT3* fusion construct was transiently expressed in *Nicotiana benthamiana* leaf epidermis. YFP:SUT3 signal was not observed on the vacuole side of the chloroplasts (Fig. 2). Furthermore, plasmolysis experiments clearly showed the presence of YFP:PttSUT3 in Hechtian strands characteristic of plasma membrane localization (Fig. 2). Thus, similar to the other characterized dicot group II transporters (Sauer, 2007), PttSUT3 imports Suc across the plasma membrane.

SUT3RNAi Increased the Internode Number and Decreased the Total Leaf Area

To investigate the function of PttSUT3 during secondary cell wall formation in wood, we expressed a *SUT3RNAi* construct under the control of the *P. trichocarpa GLYCOSYLTRANSFERASE43B* (*GT43B*) promoter. The *SUT3RNAi* sequence corresponds to a 140-bp fragment of the *PttSUT3* coding sequence (Supplemental Table S1). The *RNAi* sequence is also similar to *PttSUT1* but not to the other *PttSUTs*. However, *Populus SUT1* is not expressed in developing wood (Fig. 1; Payyavula et al., 2011), whereas *GT43B* is expressed during secondary cell wall formation, while the expression in other tissues is low or absent (Supplemental Fig. S2; Aspeborg et al., 2005; Lee et al., 2011). In situ hybridization with a *GT43B* probe showed specific labeling of cells undergoing secondary cell wall biosynthesis in *Populus* spp. (Zhou et al., 2007). The *GT43B* promoter-driven *SUT3RNAi*, therefore, is designed to target *SUT3* in developing wood. *Agrobacterium tumefaciens*-mediated transformation of stem

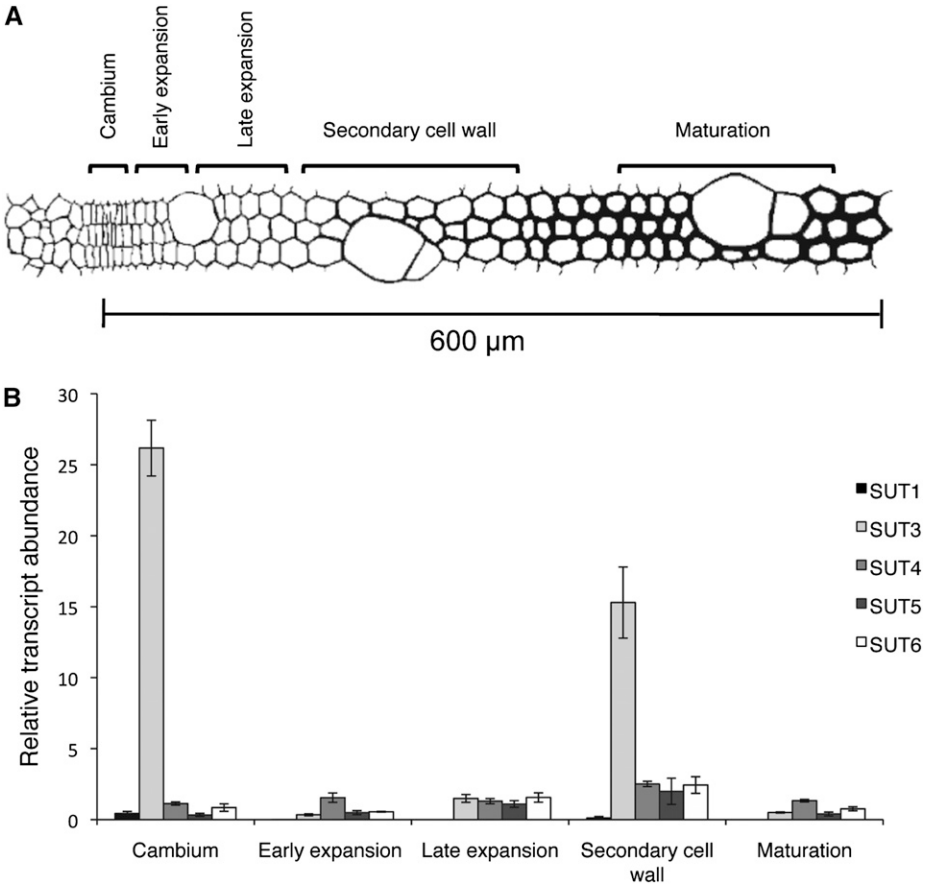

Figure 1. *PttSUT* transcript levels during wood development. A, Illustration of wood developmental zones, defined as cambium, early expansion, late expansion, secondary cell wall, and maturation, adapted from Hertzberg et al. (2001). B, Relative transcript abundance of PttSUTs in different developmental zones of developing wood. Error bars represent SE of three biological replicates.

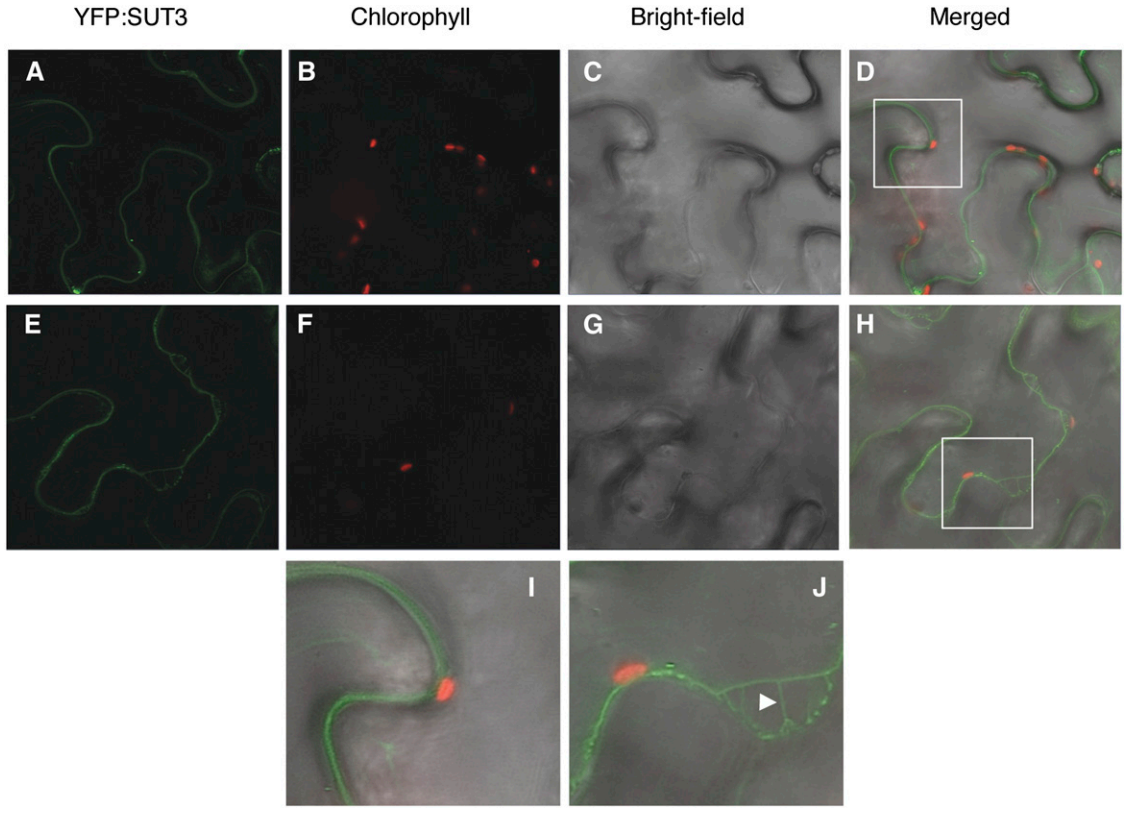

Figure 2. Subcellular localization of PttSUT3. A, YFP:PttSUT3 signal in *N. benthamiana* leaf epidermis. B, Chlorophyll autofluorescence. C, Bright-field image of epidermis. D, Merged A to C. E, YFP:PttSUT3 signal 20 min after plasmolysis in 1 M NaCl. F, Chlorophyll autofluorescence after plasmolysis. G, Bright-field image after plasmolysis. H, Merged E to H. I and J, Magnification of the selected areas (white rectangles) in D and H. I, Position of the chloroplast in relation to the YFP:SUT3 signal. J, Detachment of the plasma membrane from the cell wall accompanied by the formation of Hechtian strands (arrowhead).

pieces resulted in 18 independent *SUT3RNAi* transgenic lines. Three independent transgenic lines were selected for further characterization based on reduced *PttSUT3* transcript levels in the stems of in vitro-grown trees. The lines were amplified from cuttings, named *SUT3RNAi* line 1, line 2, and line 3, and used in all subsequent experiments.

SUT3RNAi lines and the corresponding wild type were grown on soil under greenhouse conditions for 8 weeks. qPCR analysis of *PttSUT3* transcript levels in developing wood showed that the expression of *PttSUT3* was reduced to 40% to 46% of the wild-type level in the transgenic trees (Fig. 3). The developing wood used for RNA isolation also included cambium, where the *SUT3* expression is expected to be high (Fig. 1) but where *GT43B*::*SUT3RNAi* was expected not to be expressed. Hence, the reduction in *PttSUT3* expression during secondary cell wall formation may be more pronounced than indicated by the qPCR results.

The greenhouse-grown 2-month-old *SUT3RNAi* lines showed a moderate but significant reduction in height as well as stem thickness compared with the wild type (Fig. 4A; Table I). There was also a clear decrease in the rate of leaf growth in the *SUT3RNAi* lines, resulting in approximately 50% reduction in final leaf size (Fig. 4C). The difference in leaf size was less pronounced in young leaves but started to increase after leaf 7 counted from the top (Fig. 4C). The linear leaf expansion phase had shifted from leaf 7 to leaf 13 in the wild type from leaf 9 to leaf 15 in *SUT3RNAi* (Fig. 4C). Hence, the duration of the leaf expansion phase was similar between the wild type and *SUT3RNAi*, but the rate of leaf expansion was decreased, resulting in smaller leaves. The average number of internodes per stem length increased from 0.3 internodes per centimeter in the wild type to 0.4 internodes per centimeter in the *SUT3RNAi* lines (Table I). Hence, the effect of smaller leaves on the total photosynthetic area was partly alleviated by the increase in internode (leaf) number.

SUT3RNAi Trees Had Thinner Wood Fiber Walls

Light microscopy and transmission electron microscopy analyses were used to investigate the effect of *SUT3RNAi* on wood anatomy. Visual inspection of transverse sections of stem 20 cm above soil revealed no obvious change in the overall anatomy of *SUT3RNAi* (Fig. 5A). All *SUT3RNAi* lines showed clearly thinner mature fiber walls compared with the wild type (Fig. 5B).

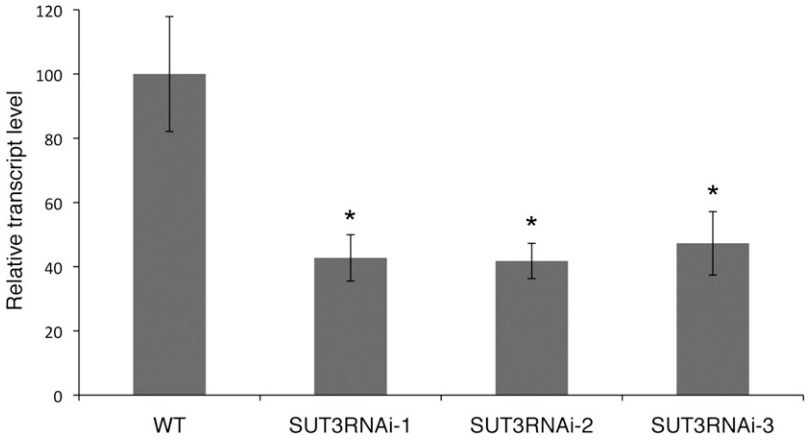

Figure 3. *PttSUT3* transcript levels in developing wood of the wild type (WT) and SUT3RNAi lines. Error bars represent SE of four biological replicates. Asterisks indicate *P* value comparison with the wild type: $*P < 0.05$ (Student's *t* test).

Quantification of the fiber wall area in four biological replicates per line confirmed this phenotype (Fig. 5C). Transmission electron microscopy images of mature fiber walls showed the difference in wall thickness to be due to thinner secondary cell wall (Fig. 6).

Comparison of mature wood fiber walls between *SUT3RNAi* and the wild type using cell-specific Fourier transform/infrared (FT-IR) microspectroscopy combined with orthogonal projection to latent structures discriminant analysis (Gorzsás et al., 2011) showed a difference in the fiber wall chemotype in all lines (Supplemental Fig. S3). The major differences in the FT-IR spectra of the *SUT3RNAi* lines included a decrease in the intensity of the –C=O vibration at around 1,740 cm^{-1} (Supplemental Fig. S3). Since cellulose does not contain –C=O bonds, the source of this change is likely to be derived from hemicelluloses and/or pectins. Considering the relative amounts of major biopolymers in secondary cell walls, these changes are more likely to originate from hemicelluloses than from pectins. This was further supported by the changes observed in the spectral region of 900 to 1,100 cm^{-1}, which is dominated by various vibrations associated with carbohydrates. There was also a shift of the –C-O band from around 1,250 to 1,210 cm^{-1}, indicating more flexible, possibly less cross-linked, cell wall polymers. Moreover, bands

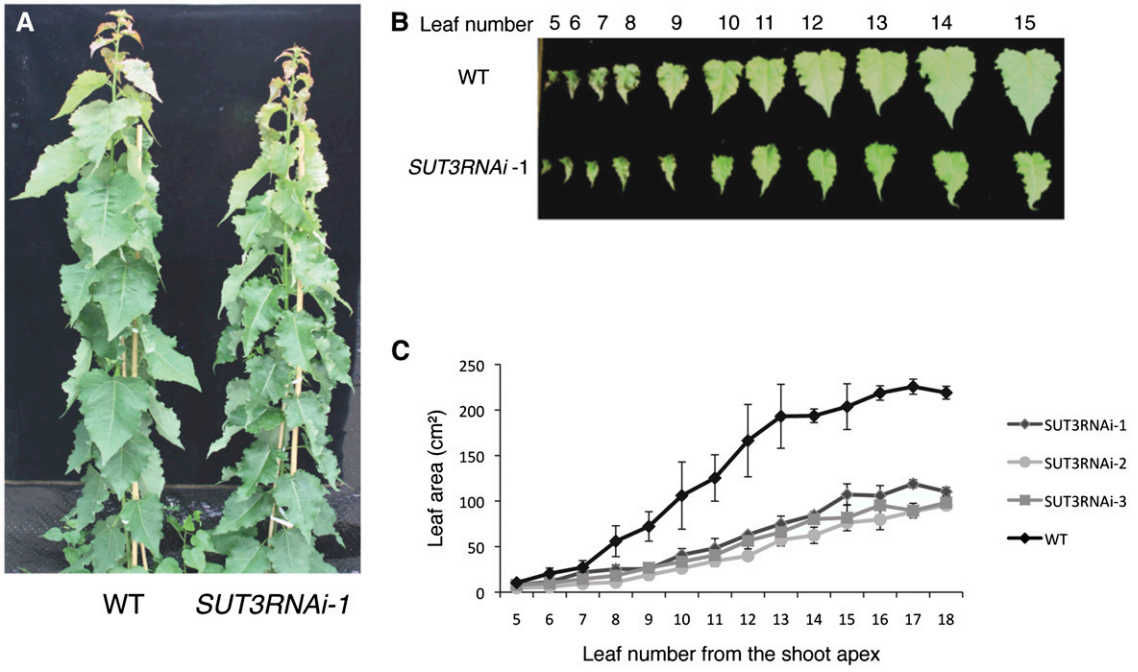

Figure 4. Phenotype of *SUT3RNAi* lines. A, Two-month-old greenhouse-grown wild-type (WT) and *SUT3RNAi* trees. B, Comparison of wild-type and *SUT3RNAi* leaves. C, Leaf area in the wild type and *SUT3RNAi*. Error bars represent SE of three biological replicates.

Table I. *Diameter, height, and internode numbers of the wild type and SUT3RNAi lines at harvest*

Values shown are means ± SE ($n = 7$ biological replicates). Student's *t* test *P* values are denoted with asterisks: $^*P < 0.05$, $^{**}P < 0.01$.

Parameter	Wild Type	SUT3RNAi-1	SUT3RNAi-2	SUT3RNAi-3
Stem diameter (mm)	12.3 ± 0.3	11.3 ± 0.4*	10.6 ± 0.1**	11.3 ± 0.3*
Stem height (cm)	178 ± 1.7	167 ± 2.3**	153 ± 2.8**	161 ± 1.7**
Internode number	58 ± 2	67 ± 2**	59 ± 3	63 ± 2**
Average number of internodes per cm	0.3 ± 0.005	0.4 ± 0.007**	0.4 ± 0.004**	0.4 ± 0.004**

associated with lignin (aromatic -C=C- vibrations at 1,510 and 1,595 cm^{-1}) showed significant changes, also pointing toward a less cross-linked structure in the *SUT3RNAi* lines (decreased 1,510:1,595 band ratio; Zhong et al., 2000). However, it is unclear from the FT-IR spectra whether the observed cross-linking changes are attributable to lignin alone or originate from changes in the cross links between lignin and cell wall carbohydrates.

To further investigate how cell wall biosynthesis was affected in *SUT3RNAi* lines, the proportions of the main wall polymers in extractive and starch-free wood were quantified in lines 1 and 3. Klason lignin analysis revealed a small but significant increase in the proportion of lignin in both RNA interference lines (Fig. 7A). Updegraff cellulose analysis (Updegraff, 1969) showed a slight, albeit statistically nonsignificant, decrease in the proportion of cellulose for lines 1 and 3 (Fig. 7B). Analysis of cell wall monosugars revealed a significant decrease in total cell wall monosugars in line 1, which was due to a decrease in mannose and galacturonic acid (Fig. 7C). However, this decrease was not observed in line 3. When estimating the amount of carbon allocated to wood, it is often more meaningful to normalize cell wall data against wood volume rather than dry weight. Hence, to estimate whether the amount of cellulose and lignin per volume of wood was reduced, the wood bulk density was first measured and defined as dry weight per wet volume. Wood density was decreased in line 1 by approximately 12% and in line 3 by approximately 7% compared with the wild type (Table II). Using the density values to derive the cellulose and lignin amounts per volume of wood revealed a clear cellulose reduction in both transgenic lines, while lignin was slightly increased (Fig. 7D).

Differences in wood density may be caused by changes in overall lumen-to-cell wall ratio. Such changes, for example, may occur as a result of altered vessel-to-fiber ratio, differences in cell number, or the morphology of xylem cells. No difference in the number of fibers or in the relative fiber area between the wild type and *SUT3RNAi* lines 1 and 3 was observed (Table II). Hence, the reduced wood density in *SUT3RNAi* was most likely due to a reduction in the fiber cell wall thickness and a corresponding increase in fiber lumen size.

In summary, *SUT3RNAi* reduced the wood density and thickness of the secondary cell walls of wood fibers, and this was accompanied by a decrease in cellulose and an increase in lignin. In addition, the FT-IR analysis indicated a changed fiber wall structure in all transgenic lines.

SUT3RNAi Had No Effect on CO_2 Assimilation

Reduced levels of group II *SUT* transcripts have been associated with reduced photosynthesis in tobacco (Burkle et al., 1998). Several reports have also shown a positive correlation between sink strength and the photosynthetic efficiency of source leaves in several plant species, including soybean (*Glycine max*), sugarcane (*Saccharum officinarum*), and *Populus* spp. (Clough et al., 1981; McCormick et al., 2006; Coleman

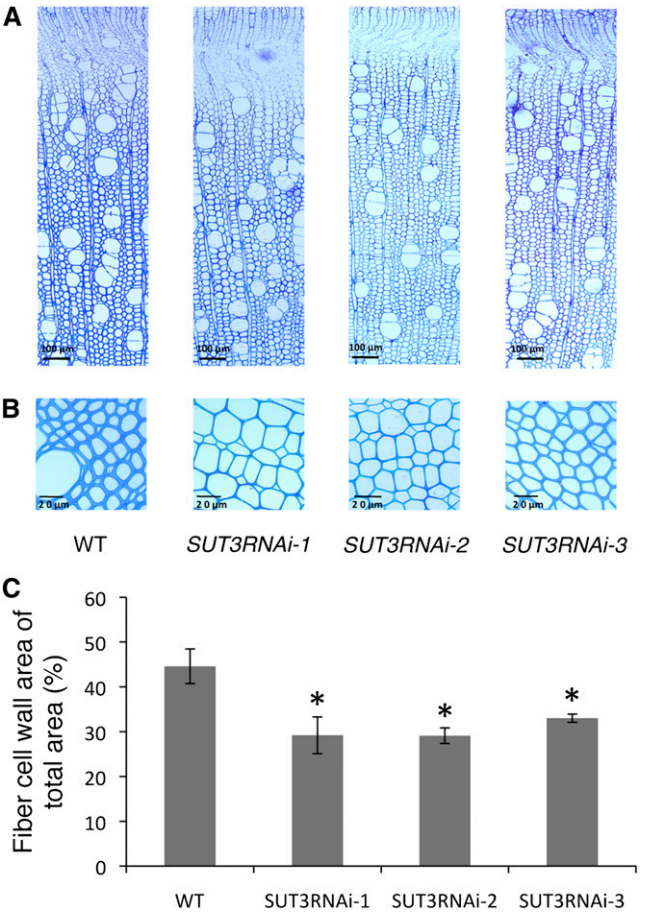

Figure 5. Wood anatomy and fiber wall area in the wild type (WT) and *SUT3RNAi* lines. A and B, Light microscopy images of representative stem sections. C, Fiber cell wall area of mature xylem fiber cells. Error bars represent SE of four biological replicates. Asterisks indicate *P* value comparison with the wild type: $^*P < 0.05$ (Student's *t* test). [See online article for color version of this figure.]

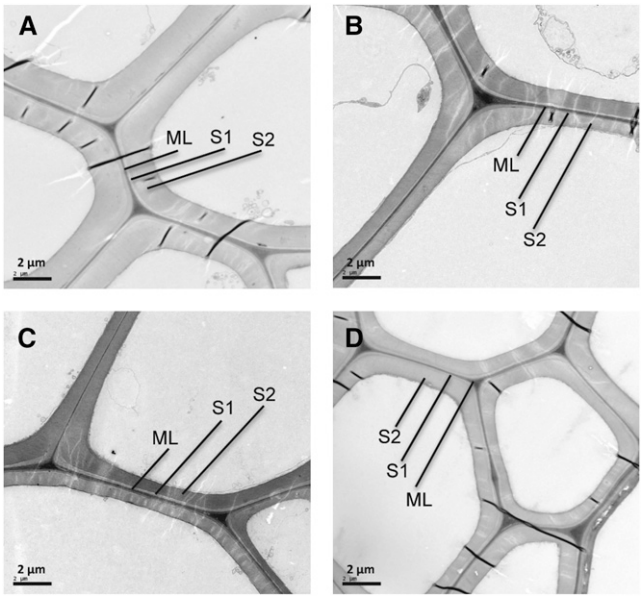

Figure 6. Transmission electron microscopy images of representative mature wood fiber walls in the wild type (A), *SUT3RNAi*-1 (B), *SUT3RNAi*-2 (C), and *SUT3RNAi*-3 (D). Cell wall layers are indicated as middle lamella (ML), S1, and S2.

et al., 2008). These observations raised the possibility that the *SUT3RNAi* wood phenotype could be due to general carbon limitation. To investigate this, we measured the source leaf CO_2 assimilation rate under different photosynthetic active-light intensities. No difference between *SUT3RNAi* lines and the wild type was observed (Supplemental Fig. S4), establishing that reduced photosynthetic efficiency was not the cause of the observed wood phenotype. However, it remained possible that the reduction in source leaf size in *SUT3RNAi* (Fig. 4) may have reduced the amount of carbon available for wood biosynthesis.

Specific Reduction of Carbon Allocation to Fiber Walls in *SUT3RNAi*

To further elucidate how *SUT3RNAi* was inhibiting carbon allocation to wood secondary cell walls, we first measured the levels of Suc, Glc, and Fru in phloem and developing wood. No significant difference in any of the sugars was observed in the phloem (Fig. 8A). In developing wood, line 3 exhibited decreased Glc and Fru levels (Fig. 8B), which could suggest reduced carbon flux from Suc to the hexose pools. Line 1 showed an increase in the Suc level in developing wood, and although not significant, this may explain why no reduction in the total Glc and Fru pool was observed in this line. When the Suc-to-hexose ratio was compared, all of the *SUT3RNAi* lines showed an increase in developing wood (Fig. 8C).

Analysis of the soluble sugar pool sizes gives limited information on the status of carbon flux into developing wood. Therefore, to gain a better understanding of how *SUT3RNAi* is affecting carbon allocation at the whole-tree level, we developed a $^{13}CO_2$ isotope-labeling system to study carbon allocation from photosynthetic tissues to developing wood. In this experiment, 8-week-old greenhouse-grown trees were placed in a sealed transparent plastic tent with controlled temperature and supplied a pulse of $^{13}CO_2$ followed by sampling in ambient CO_2. After $^{13}CO_2$ assimilation, part of the ^{13}C is exported to the developing wood, presumably mostly in the form of Suc. Hence, the measurement of ^{13}C amount in developing wood after $^{13}CO_2$ assimilation can be used to estimate carbon import to developing wood. To do this, the amount of ^{13}C in the total ethanol-soluble fraction of developing wood was quantified using elemental analyzer-isotope ratio mass spectrometry. We first established a suitable $^{13}CO_2$ incubation time and the time it took for ^{13}C isotope label to reach the developing wood in wild-type trees. A 4-h $^{13}CO_2$ pulse and sampling at 0, 4, 8, and 12 h showed that the ^{13}C was detected in the developing wood after 4 h and continued to accumulate at least until 12 h (data not shown). An 8-h time frame, therefore, was deemed suitable for the comparison of ^{13}C translocation rate between wild-type and *SUT3RNAi* trees.

SUT3RNAi and wild-type trees were given a 4-h pulse of $^{13}CO_2$, and samples were harvested at 0, 4, and 8 h. Interestingly, all of the *SUT3RNAi* lines accumulated more ^{13}C in the soluble fraction of developing wood compared with the wild type. This ^{13}C accumulation was apparent in lines 1 and 3 after 4 h and in all lines after 8 h, with lines 1 and 3 showing significant label accumulation (Fig. 9).

In summary, the unchanged total Suc pool in developing wood and the ^{13}C accumulation in the ethanol-soluble fraction suggested that Suc transport into the developing wood of the *SUT3RNAi* lines was not limiting. Instead, the incorporation of carbon from the soluble fraction into secondary cell walls was reduced, as shown by the thinner wood fiber walls. A likely explanation for this observation is that the Suc import into the secondary cell wall-forming cells was inhibited in the *SUT3RNAi* lines.

DISCUSSION

Molecular mechanisms of carbon allocation to wood are poorly understood, but they are likely to involve active transport of sugars. Suc is the main transported form of carbon in several trees, and SUTs responsible for the proton gradient-driven transport of Suc have been identified from several tree species, including *Betula pendula* (Wright et al., 2000), *Juglans regia* (Decourteix et al., 2006), and *Populus* spp. (Payyavula et al., 2011). Here, we investigated the role of SUTs in carbon import into secondary cell wall-forming wood fibers of aspen.

Transcript profiling of the *SUT* gene family across developing wood indicated a role for *PtSUT3* in cambium and during secondary cell wall formation (Fig. 1).

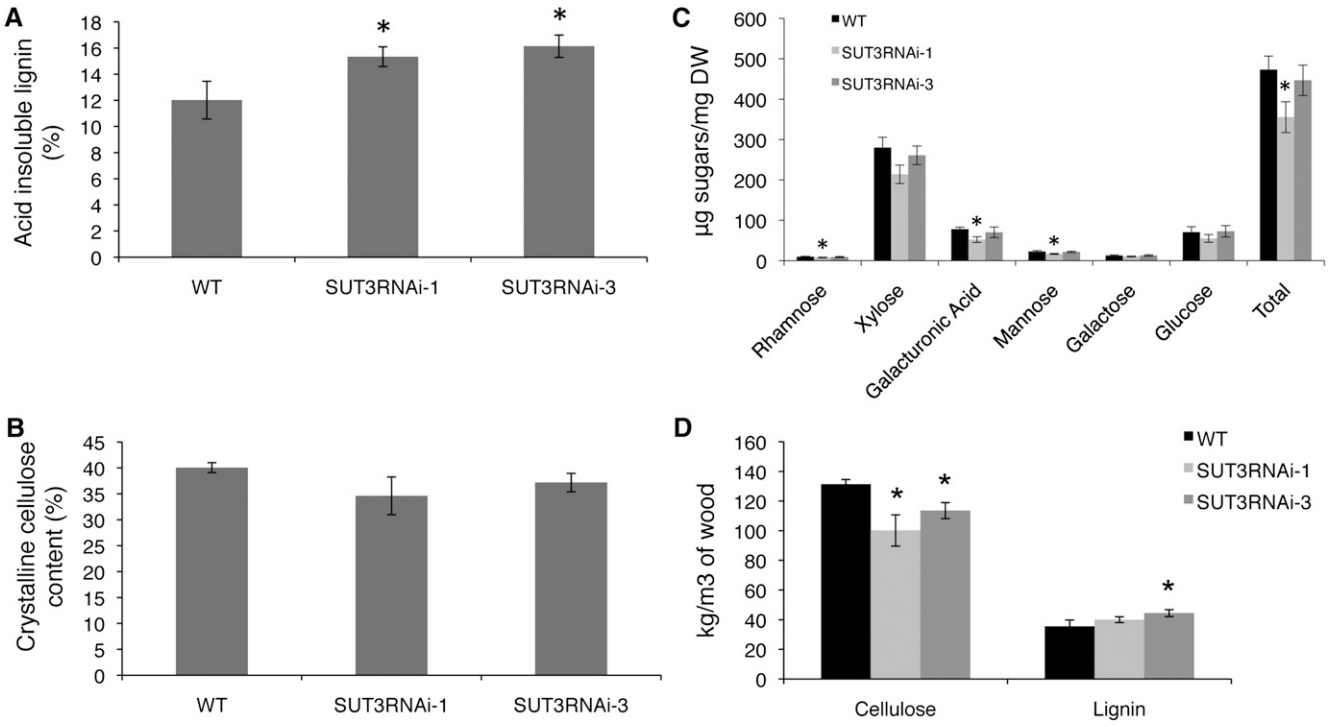

Figure 7. Analysis of extractive and starch-free wood in the wild type (WT) and *SUT3RNAi* lines. A, Acid-insoluble lignin. B, Crystalline cellulose. C, Cell wall monosugars. DW, Dry weight. D, Estimation of cellulose and lignin content per volume of wood. Error bars represent SE of four biological replicates. Asterisks indicate *P* value comparison with the wild type: $*P < 0.05$ (Student's *t* test).

The high cambial *PtSUT3* transcript levels correlated with fast-dividing cambial cells requiring Suc for the biogenesis of new cells. In the early and late expansion zones, xylem cells undergo primary wall biosynthesis and turgor pressure-driven growth (Mellerowicz et al., 2001), and during this stage, the *PtSUT3* transcript levels decreased relative to cambium. A clear increase in *PtSUT3* transcript levels was observed during secondary cell wall formation, when the majority of the wood biomass is formed, and the levels decreased again toward the maturation and cell death zone (Fig. 1). Thus, *PtSUT3* transcript levels in developing wood correlated with carbon demand for radial growth.

To investigate the function of PttSUT3 during secondary cell wall biosynthesis in wood, we used the promoter of *GT43B* to drive the expression of a *SUT3RNAi* construct. We reasoned that the use of the *GT43B* promoter for *SUT3RNAi* expression was likely to prevent substantial effects on cambial *PttSUT3* expression, which may have led to severe growth phenotypes. Three independent *SUT3RNAi* lines with 40% to 46% remaining *PttSUT3* transcript in developing wood were selected for characterization. The reduction in *PttSUT3* transcripts correlated with the reduced fiber wall area in all *SUT3RNAi* lines (Fig. 5). Thinner secondary walls of fibers are a reliable indicator of reduced carbon allocation to wood. A similar phenotype was observed in transgenic hybrid aspen with reduced wood fructokinase activity, which led to a reduction in cellulose (Roach et al., 2012). We also observed reduced cross-linking of fiber wall polymers in *SUT3RNAi* by FT-IR, possibly caused by changes in the cell wall polymer proportions.

Quantification of extractive free wood polymer proportions per dry weight showed a significant increase in lignin accompanied by a tendency to decreased cellulose in *SUT3RNAi* (Fig. 7, A and B). The changes in the proportions of wood cell wall polymers were most

Table II. *Wood bulk density, fiber area, and number of fiber cells per 10,000 μm^2 in the wild type and SUT3RNAi lines*

Values shown are means ± SE ($n = 4$ biological replicates). Student's *t* test *P* values are denoted with asterisks: $*P < 0.05$.

Parameter	Wild Type	SUT3RNAi-1	SUT3RNAi-3
Bulk density (kg m^{-3})	295 ± 6	260 ± 11*	275 ± 10
Fiber area of total area (%)	80 ± 0.9	78 ± 0.6	79 ± 0.4
Number of fiber cells per 10,000 μm^2	58 ± 3	58 ± 3	59 ± 3

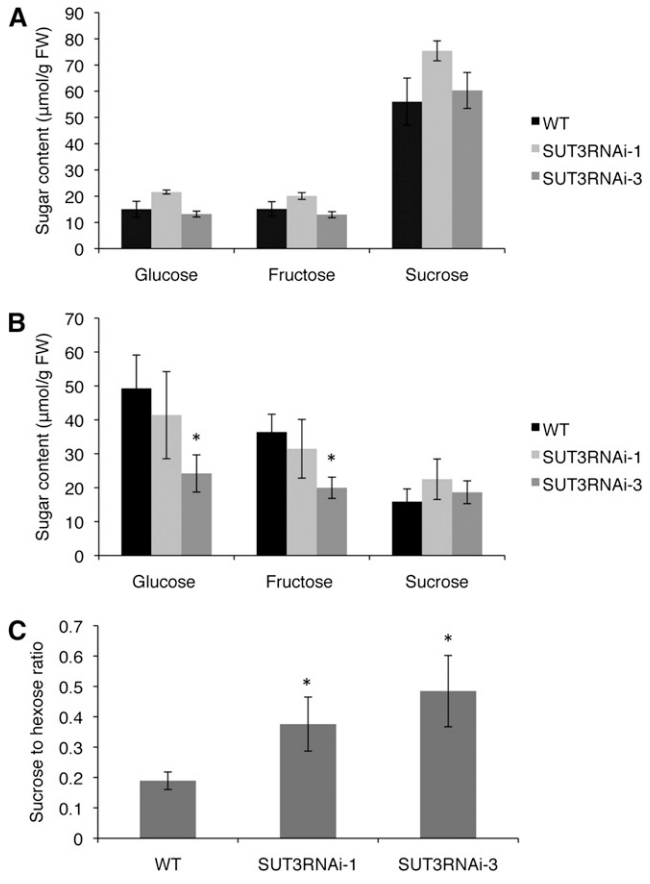

Figure 8. A and B, Analysis of Suc, Glc, and Fru content in phloem (A) and in developing wood (B) of the wild type (WT) and *SUT3RNAi* lines. FW, Fresh weight. C, Suc-to-hexose ratio in developing wood. Error bars represent SE of four biological replicates. Asterisks indicate *P* value comparison with the wild type: $*P < 0.05$ (Student's *t* test).

likely reflecting the primary effect of *SUT3RNAi* on the carbohydrate fraction of secondary cell walls: the amount of lignin per gram of dry weight increased when cellulose decreased. The nature of cell wall changes became more obvious when the decrease in the *SUT3RNAi* wood density was taken into consideration. Per volume of wood, *SUT3RNAi* lines clearly contained less cellulose, whereas lignin content was modestly increased (Fig. 7D). Carbon for lignin biosynthesis is also derived from the imported Suc; however, lignification continues in the maturation/cell death zone, where *SUT3* expression is low and *SUT3RNAi* is expected not to be active (Fig. 1; Supplemental Fig. S2). At this stage, carbon for lignin may be supplied by ray cells, which remain alive in the maturation/cell death zone. This hypothesis is supported by recent evidence from *Zinnia elegans* cell culture and Arabidopsis ex periments showing that lignification continues after cell death and that this process is supported by the adjacent living parenchymatic cells (Pesquet et al., 2013).

In addition to the wood fiber wall phenotypes, the height and diameter growth of *SUT3RNAi* lines was modestly affected (Table I). All lines also showed a clear increase in the average number of internodes per centimeter of stem (from 0.3 to 0.4), accompanied by an approximately 50% decrease in mature leaf size (Table I; Fig. 4). Although *SUT3RNAi* was expected to be primarily active in secondary cell wall-forming cells, a direct effect on young leaves and shoot tip cannot be excluded. A general sink role for the *J. regia* group II *SUT* (*JrSUT1*) was postulated based on high *JrSUT1* transcript levels in diverse sink tissues such as roots, female flowers, and stem, while the transcripts were barely detected in source leaves (Decourteix et al., 2006). However, qPCR analysis detected no *PtaSUT1* transcripts in shoot tip and developing leaves and only very low levels of *PtaSUT3*, arguing against a function of *Populus* spp. group II SUTs in these sink tissues (Payyavula et al., 2011). Hence, it is possible that the leaf area and number were influenced indirectly by the reduction of *PttSUT3* in developing wood. In this context, it is interesting that woody species transport significant amounts of carbon in xylem; for example, 9% to 28% of the carbon delivered to leaves in 3-month-old *Populus* spp. trees over a diurnal cycle was derived from sugars transported by the transpiration stream (Mayrhofer et al., 2004). It is possible that *SUT3RNAi* reduced the amount of carbon transported to shoot tips

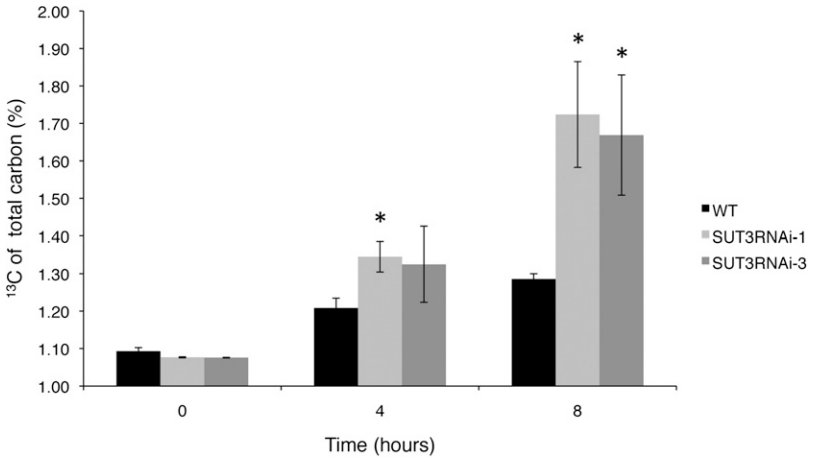

Figure 9. Accumulation of ^{13}C in the ethanol-soluble fraction of developing wood in 2-month-old trees labeled with $^{13}CO_2$. $^{13}CO_2$ was supplied for 4 h, and samples were harvested at 0, 4, and 8 h after the start of the labeling. Error bars represent SE of three biological replicates. Asterisks indicate *P* value comparison with the wild type (WT): $*P < 0.05$ (Student's *t* test).

and growing leaves in the transpiration stream. However, further experiments are needed to investigate how *SUT3RNAi* affected internode number and leaf area.

The shoot growth phenotypes complicated the interpretation of the *SUT3RNAi* effect, since a decrease in photosynthetic area may have reduced the amount of carbon available for wood secondary cell wall biosynthesis. However, we did not observe significant differences in Suc levels in the developing wood (Fig. 8), suggesting that Suc was not limiting. Reduced group II *SUT* expression has been shown to result in reduced CO_2 assimilation in tobacco (Burkle et al., 1998), raising the possibility that the carbon flux to wood may have been reduced in *SUT3RNAi*, even though the wood Suc pool size was similar to that in the wild type. However *SUT3RNAi* had no effect on the rate of CO_2 assimilation (Supplemental Fig. S4), and $^{13}CO_2$ pulse-chase experiments showed increased ^{13}C accumulation in developing wood in the *SUT3RNAi* lines, showing that Suc movement from photosynthetic tissues into developing wood was not constrained (Fig. 9). Together with the observed thinner fiber walls and reduced wood density, the accumulation of ^{13}C in the soluble extract of the *SUT3RNAi* wood was likely due to reduced Suc transport into secondary cell wall-forming cells.

Lateral Suc transport in developing wood is thought to occur symplasmically in the ray cells, as discussed in the introduction. Solute transport in rays has been hypothesized to be facilitated by cytoplasmic streaming propelled by cytoskeletal components, including microtubules, microfilaments, and myosin (Chaffey and Barlow, 2001), and therefore may be independent of SUT activity. The YFP:PttSUT3 localized to the plasma membrane in epidermal cells of tobacco leaves in a transient expression assay (Fig. 2), supporting a model where PttSUT3 is responsible for Suc import across the plasma membrane during secondary cell wall formation in developing wood. The mechanism of Suc export from plant cells was recently revealed by the identification of SUCROSE EFFLUX CARRIERS (SWEETs) in Arabidopsis (Chen et al., 2012). The *Populus* spp. genome encodes for 31 SWEETs, some of which are expressed in developing wood (A. Mahboubi and T. Niittylä, unpublished data). Hence, the current model of apoplasmic Suc transport between neighboring cells (Braun, 2012) suggested that the *Populus* spp. SWEETs are responsible for Suc export from ray cells followed by SUT3-mediated Suc import into fibers undergoing secondary cell wall formation. In the future, it will be important to localize the PttSUT3 in developing wood to test this hypothesis. The possibility of symplasmic connections between ray cells and developing vessels/fibers also needs further investigation to assess the possible contribution of symplasmic transport.

Nonetheless, our results suggested that symplasmic transport or apoplasmic Suc cleavage followed by hexose sugar import into the secondary cell wall-forming wood fibers was unable to compensate for the reduction in *PttSUT3* levels. Hence, based on the presented data, it is concluded that PttSUT3 imports carbon into the secondary cell wall-forming wood fibers, making this SUT a critical component in the wood formation of trees.

MATERIALS AND METHODS

Plant Material and Growth Conditions

Transgenic and wild-type hybrid aspen (*Populus tremula* × *Populus tremuloides*) trees were micropropagated, grown in vitro for 4 weeks, and then transferred to soil. Trees were grown in the greenhouse at 20°C/15°C (light/dark) with 50% to 70% humidity and an 18-h-light/6-h-dark photoperiod. Approximately 1 L of 0.2% Rika-S fertilizer (nitrogen:phosphorus:potassium, 7:1:5; Weibulls Horto; http://www.weibullshorto.se) was applied every 7 d. Trees were harvested after 10 weeks in the greenhouse, and samples were frozen in liquid nitrogen and stored in −80°C. Developing wood used for gene expression, soluble sugar, and ^{13}C isotope analyses was obtained by peeling the bark and scraping the wood tissues from the bottom one-third of the stem excluding the section 0 to 20 cm above the soil. The phloem sample for sugar analysis was collected by scraping the inside of the pealed bark from the same stem section. The remaining wood was cleaved to remove the pith, freeze dried, and used for wet chemistry analysis. Sections for anatomy, fiber wall area, and FT-IR measurements were prepared from stem 20 cm above the soil.

Samples for *SUT* family transcript level analysis in different wood developmental zones were harvested from three 45-year-old aspen (*Populus tremula*) trees on July 7, 2010, at Mullkälen, Sweden. Trees were cut with a motor saw, and stem pieces were frozen in liquid nitrogen. Sections were made from different wood developmental zones (cambial, early expansion, late expansion, developing xylem, and maturation/cell death zones) as described previously (Hertzberg et al., 2001).

SUT3RNAi Vector Construction and Hybrid Aspen Transformation

The RNA interference cassette was created in the pBluescript SK+ vector using a 140-bp fragment of *PttSUT3* in the sense and antisense orientations. The RNA interference cassette was then inserted into the pENTR-D-TOPO entry vector (Invitrogen; www.invitrogen.com) and moved into the pK2GW7 destination vector (Karimi et al., 2002), where the 35S promoter was replaced by a 1,490-bp promoter fragment of *Populus trichocarpa GL43B*. Hybrid aspen was transformed as described by Nilsson et al. (1992).

Subcellular Localization of PttSUT3

The coding sequence of *PttSUT3* was cloned into the pB7WGY2 binary vector (Karimi et al., 2002). Transient tobacco (*Nicotiana tabacum*) leaf *Agrobacterium tumefaciens*-mediated transformation was performed as described (Sparkes et al., 2006), and yellow fluorescent protein fluorescence was imaged with a Leica SP2 confocal microscope (http://www.leica-microsystems.com).

Growth Analysis

For stem height, the distance from the bottom of the stem to the shoot tip was measured. The stem diameter was measured 20 cm above the soil. The number of internodes was counted from the first visible internode to the internode 20 cm above the soil. The leaf area was measured using ImageJ software (rsbweb.nih.gov) from scaled leaf photographs.

Transcript Analysis

Quantitative real-time PCR was used for transcript abundance analysis. To assess the transcript levels of all hybrid aspen *SUTs* along the wood developmental zones, tangential sections were made from different wood developmental stages using a cryotome. Total RNA was extracted from the sections using the miRNeasy Micro Kit (Qiagen; www.qiagen.com) with on-column DNase (Qiagen) treatment. One hundred nanograms of total RNA was amplified using the MessageAmp Premier RNA Amplification Kit (Ambion; http://www.invitrogen.com/ambion). The concentration of amplified RNA was adjusted to 250 ng μL^{-1}. To analyze the *SUT3* transcript abundance in developing wood of greenhouse-grown wild-type and *SUT3RNAi* lines,

developing wood including the tissue from the cambium to the cell death/maturation zone was scraped into liquid nitrogen and homogenized. RNA was isolated from the homogenized scrapings using the Plant RNeasy kit (Qiagen). qPCR was performed using the CFX96 real-time system (Bio-Rad; http://www.bio-rad.com/), and double-stranded DNA was detected with SYBRGreen (Bio-Rad). Based on the stability of expression, the 26S proteasome transcript level was used for normalization in the wood developmental series. Actin and ubiquitin transcript levels were used as reference genes in total developing wood samples. Relative transcript level was calculated using the delta quantification cycle method (Pfaffl, 2001). Gene-specific primers used for *SUT* transcript analysis are listed in Supplemental Table S1.

Wood Anatomy and Wet Chemical Analysis

For wood anatomy analysis, 1-mm cross sections were prepared from the middle of the internode located 20 cm above the ground. Sections were fixed in 3% (v/v) glutaraldehyde containing 2% (v/v) paraformaldehyde in sodium cacodylate buffer (0.1 M; pH 7.2). Fixed sections were then dehydrated through an ethanol series and embedded in LR White resin (www.agarscientific.com). Cross sections (0.5 μm) were cut using a microtome, and the sections were stained with toluidine blue. Mature wood cell wall images were recorded approximately 1 mm from the cambium using a Leica DMLB light microscope and a Leica DC300 camera (www.leicamicrosystems.com). Fiber cell wall area was calculated from the images using ImageJ software (rsbweb.nih.gov). Fiber cell number in mature wood was counted from the same images.

For cell wall polymer analysis, freeze-dried mature wood was ground to powder using a ball mill. Extractive free wood was then prepared by extraction with 70% ethanol for 30 min at 95°C, followed by chloroform:methanol (1:1) for 5 min at room temperature and two washes with acetone. To remove starch, the wood powder was then treated overnight at 37°C with 1,000 units of α-amylase (Roche; http://www.roche.com) in 0.1 M potassium phosphate buffer, pH 7. Crystalline cellulose content was determined using the Updegraff method (Updegraff, 1969) followed by an anthrone assay for the detection of released Glc (Melvin, 1953). Lignin content was measured by the Klason lignin method (Fengel and Wegener, 2003). For the quantification of hemicellulose sugars, 0.5 mg of extractive free wood was methanolyzed using 2 M HCl/methanol followed by trisil reagent (1,1,3,3,3-hexamethyldisilazane + trimethylchlorosilane + pyridine, 3:1:9) derivatization using the Sylon HTP kit (Supelco; http://www.sigmaaldrich.com) as described (Sweeley et al., 1963). The monosugar contents were then determined on a gas chromatograph-mass spectrometer (7890A/5975C; Agilent Technologies; www.agilent.com).

Wood Density Measurement

Wood density was measured on an oven dry weight per wet volume basis. Wood pieces were placed in water on an XA105 analytical balance with precision of 0.01 mg (Mettler Toledo; www.mt.com) and pushed under water to measure the sample volume based on displaced water weight. Samples were then oven dried at 102°C for 24 h and weighed again to obtain the dry mass weight. The wood density was then estimated from the dry weight-to-wet volume ratio.

Soluble Sugar Analysis

Glc, Fru, and Suc were extracted and measured as described previously by Stitt et al. (1989) and Roach et al. (2012).

$^{13}CO_2$ Labeling and ^{13}C Analysis

Two-month-old trees were enclosed in a transparent tent and labeled with 0.3 mol of $^{13}CO_2$ for 4 h at 25°C and relative humidity of 65% to 75%. The CO_2 concentration inside the chamber was between 400 and 500 μL L^{-1}, as determined by a WMA-4 CO_2 analyzer (www.ppsystems.com) calibrated for $^{13}CO_2$. The labeled trees were harvested, and the developing wood was scraped and ground in liquid nitrogen. Ethanol-soluble extract from the developing wood was dried and analyzed with an elemental analyzer isotope ratio mass spectrometer (www.thermofisher.com) to determine the ^{13}C content.

Photosynthesis Rate Measurement

The light-response curve of the photosynthesis rate was measured for wild-type and *SUT3RNAi* lines at different photon irradiances (0, 50, 100, 300, 700, 1,200, 1,500, and 1,800 μmol s^{-1} m^{-2}) using the Li-Cor portable gas exchange system (LI-COR 6400; http://www.licor.com).

Supplemental Data

The following materials are available in the online version of this article.

Supplemental Figure S1. Anatomy and viability staining of developing wood used for transcript profiling of *PtSUTs*.

Supplemental Figure S2. Expression of *GT43B* in hybrid aspen.

Supplemental Figure S3. FT-IR analysis of mature wood fiber walls.

Supplemental Figure S4. Analysis of the photosynthesis rate in the wild type and *SUT3RNAi*.

Supplemental Table S1. List of primers and the *SUT3RNAi* sequence.

ACKNOWLEDGMENTS

We thank Kjell Olofsson and Lenore Johansson for help with sample preparation and microscopy, Junko Takahashi-Schmidt for help with the wood wet chemistry analysis, and Stephanie Robert for assistance with the confocal microscope.

Received August 27, 2013; accepted October 29, 2013; published October 29, 2013.

LITERATURE CITED

Aspeborg H, Schrader J, Coutinho PM, Stam M, Kallas A, Djerbi S, Nilsson P, Denman S, Amini B, Sterky F, et al (2005) Carbohydrate-active enzymes involved in the secondary cell wall biogenesis in hybrid aspen. Plant Physiol **137:** 983–997

Barnett JR (1981) Secondary xylem development. *In* JR Barnett, ed, Xylem Cell Development. Castle House Publications, Tunbridge Wells, England, pp 47–95

Barnett JR, Harris JM (1975) Early stages of bordered pit formation in radiata pine. Wood Sci Technol **9:** 233–241

Braun DM (2012) SWEET! The pathway is complete. Science **335:** 173–174

Burkle L, Hibberd JM, Quick WP, Kuhn C, Hirner B, Frommer WB (1998) The H^+-sucrose cotransporter NtSUT1 is essential for sugar export from tobacco leaves. Plant Physiol **118:** 59–68

Chaffey N, Barlow P (2001) The cytoskeleton facilitates a three-dimensional symplasmic continuum in the long-lived ray and axial parenchyma cells of angiosperm trees. Planta **213:** 811–823

Chen LQ, Qu XQ, Hou BH, Sosso D, Osorio S, Fernie AR, Frommer WB (2012) Sucrose efflux mediated by SWEET proteins as a key step for phloem transport. Science **335:** 207–211

Clough JM, Peet MM, Kramer PJ (1981) Effects of high atmospheric CO_2 and sink size on rates of photosynthesis of a soybean cultivar. Plant Physiol **67:** 1007–1010

Coleman HD, Samuels AL, Guy RD, Mansfield SD (2008) Perturbed lignification impacts tree growth in hybrid poplar: a function of sink strength, vascular integrity, and photosynthetic assimilation. Plant Physiol **148:** 1229–1237

Davidson A, Keller F, Turgeon R (2011) Phloem loading, plant growth form, and climate. Protoplasma **248:** 153–163

Decourteix M, Alves G, Brunel N, Améglio T, Guillio A, Lemoine R, Pétel G, Sakr S (2006) JrSUT1, a putative xylem sucrose transporter, could mediate sucrose influx into xylem parenchyma cells and be up-regulated by freeze-thaw cycles over the autumn-winter period in walnut tree (*Juglans regia* L.). Plant Cell Environ **29:** 36–47

Endler A, Meyer S, Schelbert S, Schneider T, Weschke W, Peters SW, Keller F, Baginsky S, Martinoia E, Schmidt UG (2006) Identification of a vacuolar sucrose transporter in barley and Arabidopsis mesophyll cells by a tonoplast proteomic approach. Plant Physiol **141:** 196–207

Fengel D, Wegener G (2003) Wood: Chemistry, Ultrastructure, Reactions. Reprint Kessel, Remagen, Germany

Fu QS, Cheng LL, Guo YD, Turgeon R (2011) Phloem loading strategies and water relations in trees and herbaceous plants. Plant Physiol **157:** 1518–1527

Gorzsás A, Stenlund H, Persson P, Trygg J, Sundberg B (2011) Cell-specific chemotyping and multivariate imaging by combined FT-IR microspectroscopy and orthogonal projections to latent structures (OPLS) analysis reveals the chemical landscape of secondary xylem. Plant J **66:** 903–914

Gottwald JR, Krysan PJ, Young JC, Evert RF, Sussman MR (2000) Genetic evidence for the in planta role of phloem-specific plasma membrane sucrose transporters. Proc Natl Acad Sci USA **97:** 13979–13984

Hertzberg M, Aspeborg H, Schrader J, Andersson A, Erlandsson R, Blomqvist K, Bhalerao R, Uhlén M, Teeri TT, Lundeberg J, et al (2001) A transcriptional roadmap to wood formation. Proc Natl Acad Sci USA **98:** 14732–14737

Karimi M, Inzé D, Depicker A (2002) Gateway vectors for Agrobacterium-mediated plant transformation. Trends Plant Sci **7:** 193–195

Knoblauch M, Peters WS (2010) Münch, morphology, microfluidics: our structural problem with the phloem. Plant Cell Environ **33:** 1439–1452

Kühn C, Grof CPL (2010) Sucrose transporters of higher plants. Curr Opin Plant Biol **13:** 288–298

Lalonde S, Wipf D, Frommer WB (2004) Transport mechanisms for organic forms of carbon and nitrogen between source and sink. Annu Rev Plant Biol **55:** 341–372

Langenfeld-Heyser R (1987) Distribution of leaf assimilates in the stem of Picea abies L. Trees Struct Funct **1:** 102–109

Lee CH, Teng QC, Zhong RQ, Ye ZH (2011) Molecular dissection of xylan biosynthesis during wood formation in poplar. Mol Plant **4:** 730–747

Mayrhofer S, Heizmann U, Magel E, Eiblmeier M, Müller A, Rennenberg H, Hampp R, Schnitzler JP, Kreuzwieser J (2004) Carbon balance in leaves of young poplar trees. Plant Biol (Stuttg) **6:** 730–739

McCormick AJ, Cramer MD, Watt DA (2006) Sink strength regulates photosynthesis in sugarcane. New Phytol **171:** 759–770

Mellerowicz EJ, Baucher M, Sundberg B, Boerjan W (2001) Unravelling cell wall formation in the woody dicot stem. Plant Mol Biol **47:** 239–274

Melvin SA (1953) Determination of dextran with anthrone. Anal Chem **25:** 1656–1661

Münch E (1930) Die Stoffbewegungen in der Pflanze. Gustav Fischer, Jena, Germany

Nilsson O, Alden T, Sitbon F, Little CHA, Chalupa V, Sandberg G, Olsson O (1992) Spatial pattern of cauliflower mosaic virus 35S promoter luciferase expression in transgenic hybrid aspen trees monitored by enzymatic assay and non-destructive imaging. Transgenic Res **1:** 209–220

Payyavula RS, Tay KHC, Tsai CJ, Harding SA (2011) The sucrose transporter family in Populus: the importance of a tonoplast PtaSUT4 to biomass and carbon partitioning. Plant J **65:** 757–770

Pesquet E, Zhang B, Gorzsás A, Puhakainen T, Serk H, Escamez S, Barbier O, Gerber L, Courtois-Moreau C, Alatalo E, et al (2013) Non-cell-autonomous postmortem lignification of tracheary elements in *Zinnia elegans*. Plant Cell **25:** 1314–1328

Pfaffl MW (2001) A new mathematical model for relative quantification in real-time RT-PCR. Nucleic Acids Res **29:** e45

Riesmeier JW, Willmitzer L, Frommer WB (1994) Evidence for an essential role of the sucrose transporter in phloem loading and assimilate partitioning. EMBO J **13:** 1–7

Roach M, Gerber L, Sandquist D, Gorzsás A, Hedenström M, Kumar M, Steinhauser MC, Feil R, Daniel G, Stitt M, et al (2012) Fructokinase is required for carbon partitioning to cellulose in aspen wood. Plant J **70:** 967–977

Sauer N (2007) Molecular physiology of higher plant sucrose transporters. FEBS Lett **581:** 2309–2317

Sauter JJ, Kloth S (1986) Plasmodesmatal frequency and radial translocation rates in ray cells of poplar (Populus × canadensis Moench Robusta). Planta **168:** 377–380

Schneider S, Hulpke S, Schulz A, Yaron I, Höll J, Imlau A, Schmitt B, Batz S, Wolf S, Hedrich R, et al (2012) Vacuoles release sucrose via tonoplast-localised SUC4-type transporters. Plant Biol (Stuttg) **14:** 325–336

Sokołowska K, Zagórska-Marek B (2012) Symplasmic, long-distance transport in xylem and cambial regions in branches of Acer pseudoplatanus (Aceraceae) and Populus tremula × P. tremuloides (Salicaceae). Am J Bot **99:** 1745–1755

Sparkes IA, Runions J, Kearns A, Hawes C (2006) Rapid, transient expression of fluorescent fusion proteins in tobacco plants and generation of stably transformed plants. Nat Protoc **1:** 2019–2025

Stitt M, Lilley RM, Gerhardt R, Heldt HW (1989) Metabolite levels in specific cells and subcellular compartments of plant leaves. Methods Enzymol **174:** 518–552

Sweeley CC, Bentley R, Makita M, Wells WW (1963) Gas-liquid chromatography of trimethylsilyl derivatives of sugars and related substances. J Am Chem Soc **85:** 2497–2507

Turgeon R (1996) Phloem loading and plasmodesmata. Trends Plant Sci **1:** 418–423

Updegraff DM (1969) Semimicro determination of cellulose in biological materials. Anal Biochem **32:** 420–424

Van Bel AJE (1990) Xylem-phloem exchange via the rays: the undervalued route of transport. J Exp Bot **41:** 631–644

Van Bel AJE (2003) The phloem, a miracle of ingenuity. Plant Cell Environ **26:** 125–149

Wright DP, Scholes JD, Read DJ, Rolfe SA (2000) Changes in carbon allocation and expression of carbon transporter genes in Betula pendula Roth. colonized by the ectomycorrhizal fungus Paxillus involutus (Batsch) Fr. Plant Cell Environ **23:** 39–49

Zhong RQ, Morrison WH III, Himmelsbach DS, Poole FL II, Ye ZH (2000) Essential role of caffeoyl coenzyme A *O*-methyltransferase in lignin biosynthesis in woody poplar plants. Plant Physiol **124:** 563–578

Zhou GK, Zhong RQ, Himmelsbach DS, McPhail BT, Ye ZH (2007) Molecular characterization of PoGT8D and PoGT43B, two secondary wall-associated glycosyltransferases in poplar. Plant Cell Physiol **48:** 689–699